Dynamic communicability predicts infectiousness

Dynamic Communicability Predicts Infectiousness

Alexander V. Mantzaris and Desmond J. Higham

Abstract Using real, time-dependent social interaction data, we look at correlations between some recently proposed dynamic centrality measures and summaries from large-scale epidemic simulations. The evolving network arises from email exchanges. The centrality measures, which are relatively inexpensive to compute, assign rankings to individual nodes based on their ability to broadcast information over the dynamic topology. We compare these with node rankings based on infectiousness that arise when a full stochastic SI simulation is performed over the dynamic network. More precisely, we look at the proportion of the network that a node is able to infect over a fixed time period, and the length of time that it takes for a node to infect half the network. We find that the dynamic centrality measures are an excellent, and inexpensive, proxy for the full simulation-based measures.

1 Background and Motivation

In many social interactions, the timing of the connections is vital. Suppose A meets B today and B meets C tomorrow. This makes it possible for a message, or a disease, to pass from A to B, but not from C to A. Further, the more active B happens to be tomorrow, the more potential there is for today's A-B link to have a downstream effect. Several authors have pointed out the need to account for topological dynamics when considering disease propagation. The work in [15] considers the stages that sexually transmitted diseases (STDs) pass through when infecting subpopulations of a network, and shows that the timing in the connectivity between individuals plays a crucial role. In [10] a disease is simulated with an SI model (as we use here) and an SIR alternative, over contact networks relating to high-end prostitution. Both a static and a temporal view of the interaction data is used, and the results show that temporal effects play a key role. Epidemic simulations over temporal connectivity

Department of Mathematics and Statistics, University of Strathclyde, Glasgow, UK e-mail: alexander.mantzaris@strath.ac.uk

data are also used in [7] to explore vaccination strategies. Similarly, the spread of computer malware over temporal networks is considered in [12, 11], and strategies developed for the immunisation of key nodes. The SI framework is used in [2] to characterise the global structure of a temporal network.

From a network science perspective, it is natural to seek generic *centrality* measures that rank individual nodes according to their "importance." In the case of static network topology, there is a wealth of such measures, most of which can be traced back to the social network analysis community [4]. Devising centrality measures that apply to time-dependent networks is a more recent pursuit. The work of [14] used a shortest-path-counting approach to measure the closeness/betweeness of nodes in a time varying graph. The alternative walk-counting approach in [5] was based on a direct generalization of Katz centrality [6] to the case of time-dependent networks. A key message from [13] and [8] is that centrality measures based on a static, aggregate summary of the network will not adequately reflect the hierarchy of importance.

The question that we address in this work is

given a time-dependent network, can suitable centrality measures provide useful information about the spread of epidemics?

The question is motivated by the fact that centrality measures are typically much cheaper to compute than large-scale stochastic simulations. For this reason, we focus on the dynamic communicability approach in [5] where we can deal with all nodes simultaneously by solving a sparse linear system at each time step (that is, finding x in a matrix-vector system of the form $Ax = b$, where A has the same sparsity as the current network adjacency matrix).

In the next section we give details of the computational tasks and the data set used. Sections 3 and 4 describe the data and results, and we finish with a discussion in Section 5.

2 Methodology

We consider a fixed set of N nodes whose connections are recorded at an equally spaced set of time points $t_0 < t_1 < \cdots < t_M$. The network at each time point is undirected and unweighted, with no self loops. So, at time t_k, we can record the state of the network in the adjacency matrix $A^{[k]} \in \mathbb{R}^{N \times N}$. Here $\left(A^{[k]}\right)_{ij} = 1$ if node i has a link to node j at time t_k and $\left(A^{[k]}\right)_{ij} = 0$ otherwise.

The epidemic simulations are peformed in a stochastic SI framework. At each time point a node is either susceptible (S) or infectious (I). Once made infectious, a node cannot return to the susceptible state. We begin, at t_0, by infecting a single node. Generally, to determine the status of the nodes at time t_{k+1}, we use the following rule: for each node that was in the infectious state at time t_k, we consider all the time t_{k+1} neighbours pointed to by this node. If any such neighbour is in the

susceptible state, then it is moved into the infectious state with independent probability β. More loosely, an infectious node has a fixed probability β of transmitting the infection to each of its *current* contacts.

We measure the virulence of a node in two separate ways. After starting the infection at this node, we compute

(a)   the proportion of the network infected at the final time, t_M,
(b)   the number of time points required to infect at least half of the network.

To understand the centrality measures from [5], we need to introduce the concept of a *dynamic walk of length w from node i to node j*: this is simply any traversal from i to j along w edges that respects the arrow of time (i.e. having used an edge at time t_r, the next edge that we use must exist at time t_r or later). The ability of node i to broadcast information to node j may then be measured as the total number of dynamic walks from i to j, where a walk of length w is downweighted by the factor α^w. Here $\alpha \in (0,1)$ is a fixed parameter that reduces the influence of longer walks. In the case of a single time point, this measure reduces to the classical Katz centrality [6], which may be computed through the matrix resolvent, $(I - \alpha A)^{-1}$. Generalizing to multiple time points in this way, we arrive at the expression

$$\mathscr{Q} = \left(I - \alpha A^{[0]}\right)^{-1} \left(I - \alpha A^{[1]}\right)^{-1} \ldots \left(I - \alpha A^{[M]}\right)^{-1}, \tag{1}$$

where $\mathscr{Q}_{ij}$ measures how well node i can broadcast information to node j. To obtain a single coefficient for node i we sum over all nodes in the network to obtain the *broadcast centrality*. In practice, since we plan to use this measure to rank the nodes, it is reasonable to normalize, which avoids numerical underflow/overflow, leading to the iteration

$$\hat{\mathscr{Q}}^{[k]} = \frac{\hat{\mathscr{Q}}^{[k-1]} \left(I - \alpha A^{[k]}\right)^{-1}}{\left\| \hat{\mathscr{Q}}^{[k-1]} \left(I - \alpha A^{[k]}\right)^{-1} \right\|}, \tag{2}$$

for $k = 0, \ldots, M$, with $\hat{\mathscr{Q}}^{[-1]} = I$ and $\| \cdot \|$ representing the Euclidean matrix norm. The broadcast centrality for node i is then given by $\sum_{j=1}^{N} \left(\hat{\mathscr{Q}}^{[k]}\right)_{ij}$.

Just as in the original Katz version, this centrality measure involves a parameter, α. In order for the matrix inverses to exist, we require α to be less than

$$\alpha^{\star} := \min_{0 \leq k \leq M} \left(\rho\left(A^{[k]}\right)\right)^{-1},$$

where $\rho(\cdot)$ denotes the spectral radius. Tests in [5] indicated that the results are not sensitive to the choice of α, and in all tests here we use $\alpha = 0.9\alpha^{\star}$.

3 Data

We perform the tests on real social interaction data that records email exchanges between former Enron employees [3, 9]. There are $N = 151$ individuals, and we summarize activity into daily time slices: an undirected edge between i and j indicates that at least one email (including `cc` and `bcc`) passed between the two individuals. Figure 1 shows a plot of the static aggregate degree each day for all the nodes. Because the start date is arbitrary, we smooth out its influence by repeating
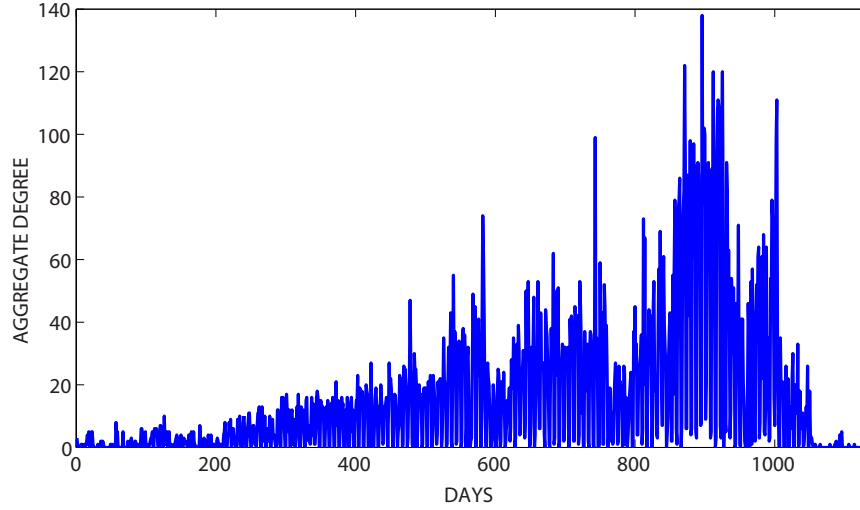

Fig. 1 The static aggregate degree each day for all of the nodes (Enron employees).

computations over a sliding window that covers half the overall period; that is, 568 of the 1036 consecutive days. So the first window runs from day 1 to day 568, the second window runs from day 2 to day 569, and so on. In this manner, we create 568 distinct evolving networks, each involving $M + 1 = 568$ consecutive days. Results are averaged over all windows.

For each of the 568 windows, we compute the broadcast centralities and, with each node in turn as a starting point for infection, perform one SI simulation. In practice we found that computing the broadcast centralities was typically an order of magnitude faster than computing $N = 151$ paths of the SI model, one from each starting state.

For a small number of windows/starting node combinations, the infection level remained below 50% at the final time point. For simplicity, these runs were omitted from the averaging process when we measured the average time to infect 50% of the population. For this reason, we regard the proportion of the network infected at the final time as the more robust of the two SI-based measures.

Table 1 Symbols for company position

President	hexagram
CEO	pentagram
Executive	pentagram
Legal	diamond
VicePresident	hexagram
DirectorofTrading	square
ManagingDirector	upward triangle
Manager	right facing triangle
Director	left facing triangle
InHouseLawyer	diamond
Trader	square
Employee	plus
Secretary	circle
all others	small dot

Table 2 Correlation coefficients relating to Figures 3, 7 and 11 for broadcast versus proportion of the network infected.

β	Pearson	Kendall Tau	Spearman
0.2	0.85	0.70	0.88
0.5	0.88	0.82	0.94
1.0	0.94	0.81	0.94

The Enron data set also provides the positions of most employees within the company. For completeness, we display this information in our figures. Table 1 indicates the symbols that we use. However, in the results that follow there does not appear to be any clear pattern based on these semantic labels.

4 Results

The SI simulations were repeated for three different choices of the infection probability, β. In each case, we provide two dimensional scatter plots (one point for each node) that compare, in a pair-wise fashion, (a) the proportion of the network infected at the final time point, (b) the time taken to infect 50% of the network, and (c) the natural logarithm of the broadcast centrality. The corresponding Pearson, Kendall Tau and Spearman correlation coeficients for the (a)-(c) pair are reported in Table 2.

We also scatter plot the aggregate degree—that is, the total number of edges involving the node over all time points—against the proportion of the network infected.

We emphasize that the broadcast centrality and aggregate degree are independent of the parameter β in the SI model.

4.1 Infection rate $\beta = 0.2$ results

For $\beta = 0.2$, Figure 2 focuses on the SI model and compares the infected proportion against the time to infect 50%. These are seen to have a strong negative correlation, and hence, in terms of ranking the nodes by infectiousness, they are broadly comparable.
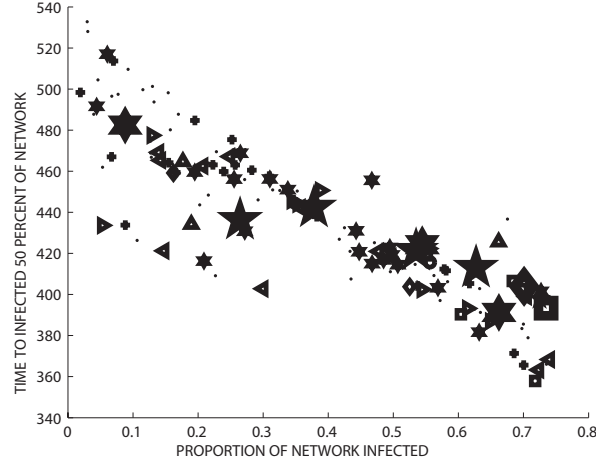

Fig. 2 Infected proportion versus time for 50% of the network to be infected for $\beta = 0.2$.

The broadcast centrality is compared with the infected proportion in Figure 3 and with the time to infect 50% in Figure 4. In both cases, we see strong correlations.

In Figure 5 we show the aggregate degree against the infection level. Although most of the very high degree nodes are typically strong infectors, the relationship is far from linear and breaks down at the lower levels. We also emphasize that the integer-valued nature of nodal degree makes it liable to produce more ties when used to rank nodes.

4.2 Infection rate $\beta = 0.5$ results

We now repeat the experiments from subsection 4.1 with a stronger infection rate of $\beta = 0.5$.

Figure 6 shows the infected proportion against the time to infect. We see that the two measures are inverseley correlated more tightly than in the $\beta = 0.2$ case, shown in Figure 2.
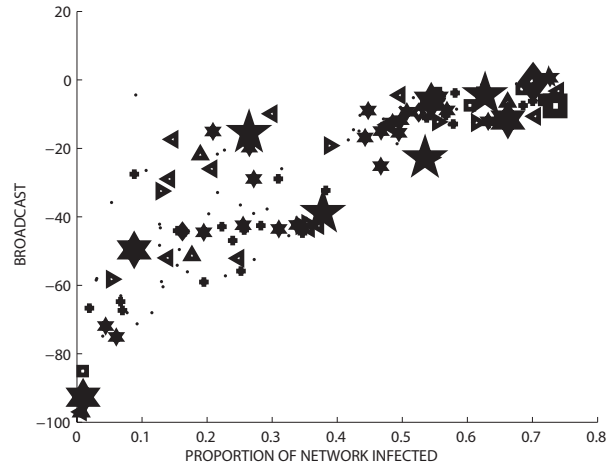
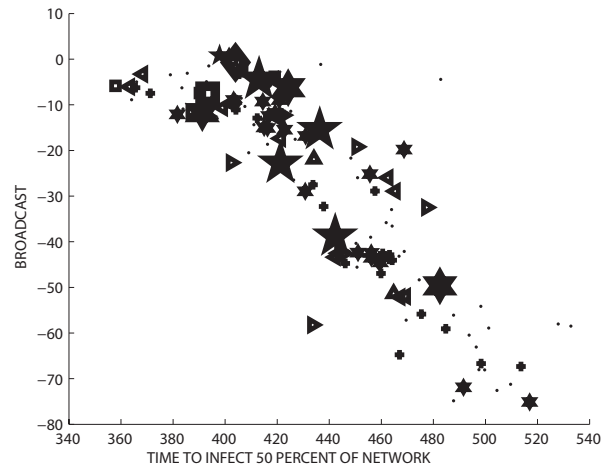**Fig. 3** Broadcast centrality versus infected proportion for $\beta = 0.2$.

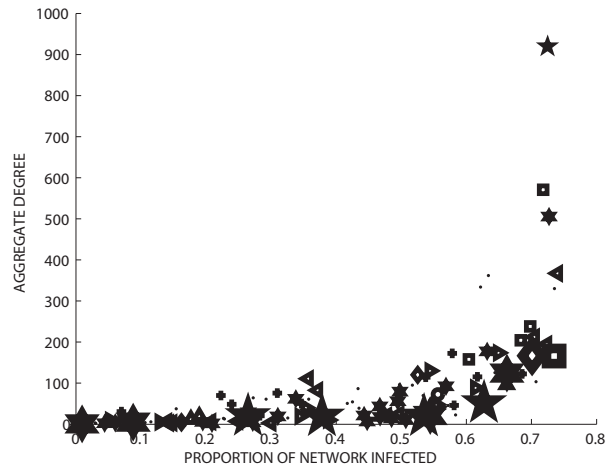**Fig. 4** Broadcast centrality versus time to reach 50% network infection for $\beta = 0.2$.

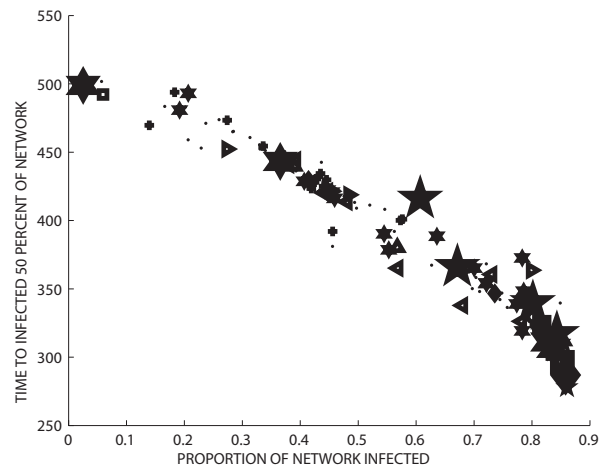**Fig. 5** Average degree versus infected percentage for $\beta = 0.2$.

Fig. 6 The infected proportion against the time for 50% of the network to be infected for $\beta = 0.5$.

Figures 7 and 8 compare the broadcast centrality with infected proportion and time to infect 50%, respectively. The performance of the broadcast measure as a proxy seems to improve slightly over the $\beta = 0.2$ case. This is confirmed in Table 2 in terms of the three correlation coefficients.
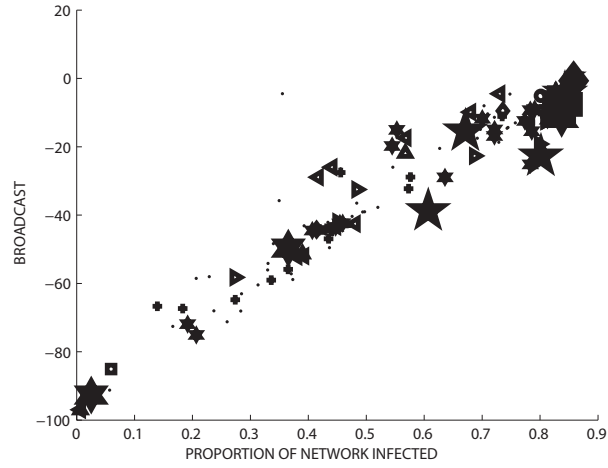

Fig. 7 Broadcast centrality versus infected proportion for $\beta = 0.5$.
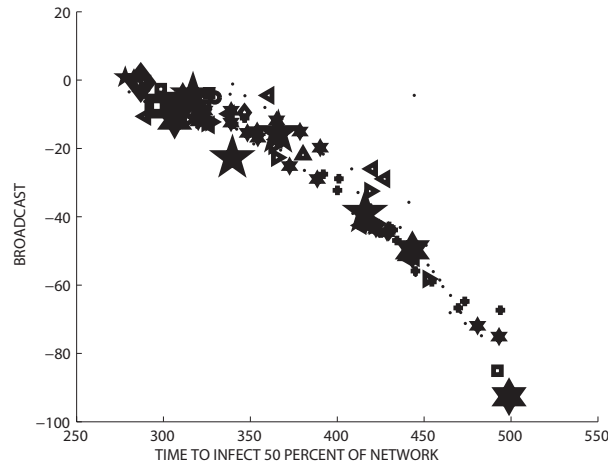

Fig. 8 Broadcast centrality versus time to reach 50% network infection for $\beta = 0.5$.

Figure 9 shows the aggregate degree against infected proportion and the effect observed for $\beta = 0.2$ is now further exaggerated.
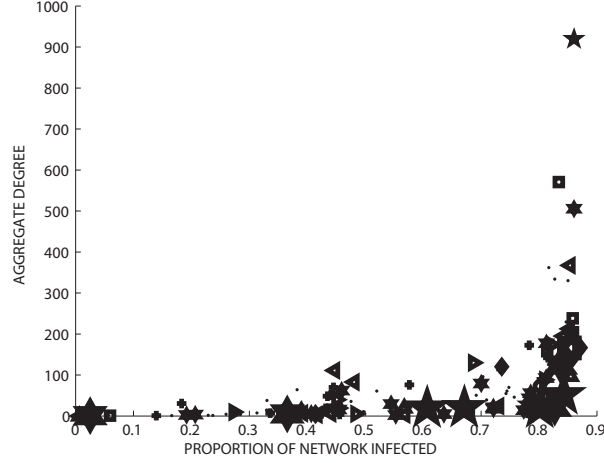

Fig. 9 Average degree versus infected proportion for $\beta = 0.5$.

4.3 Infection rate $\beta = 1.0$ results

The final set of tests uses $\beta = 1.0$ in the SI model. In this case the disease transmission is no longer stochastic.

Following the format of the previous subsections, Figure 10 shows the infected proportion against the time for 50% infection, and Figures 11 and 12 compare broadcast centrality with infected proportion and time to reach 50% network infection, respectively. In this case, looking at the SI model in isolation, we see a build up of virulent nodes in Figure 12 that have a similar ability to infect around 85-90% of the network, but vary quite considerably in their time taken to infect the first 50%. The picture is 'spoilt' by the faster infectors being unable to 'finish off' the final 10% of nodes. To some extent this behaviour is also reflected in Figure 11, where some of the very high broadcasters are underperforming in terms of their relative ability to infect a very high proportion of the network. The results in Figure 12, where broadcast is compared with time to infect 50% of the network, show a smoother relationship. We conclude that in this high-infection-rate, sparse-connectivity regime, the time to infect 50% is a more realistic measure of a node's virulence than the infected proportion after a fixed, long time horizon.
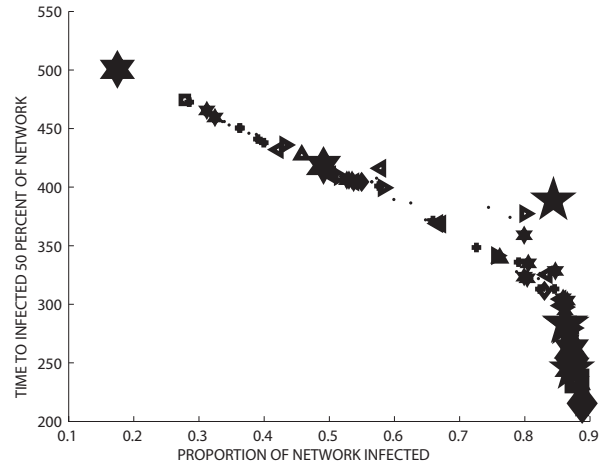
Fig. 10 Infected percentage versus time for 50% of the network to be infected for $\beta = 1.0$.
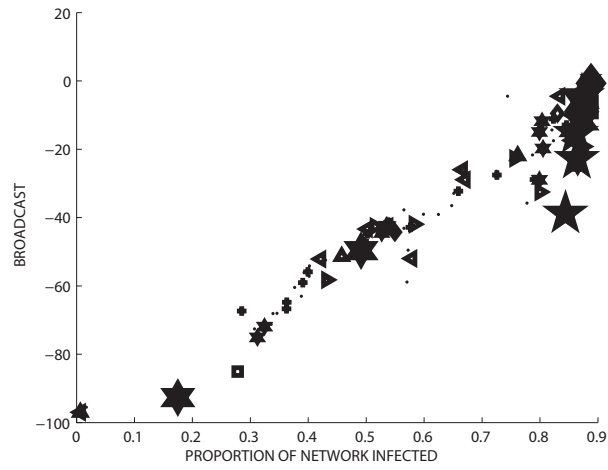

Fig. 11 Broadcast centrality versus infected proportion for $\beta = 1.0$.
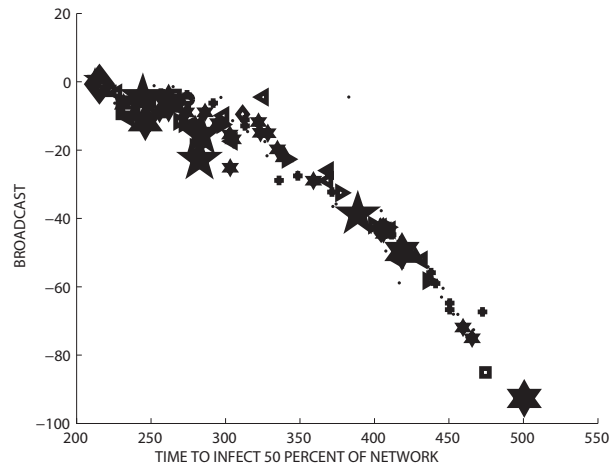
Fig. 12 Broadcast centrality versus time to reach 50% network infection for $\beta = 1.0$.

Finally, Figure 13 shows again that the aggregate degree is a poor predictor of the infected network proportion.
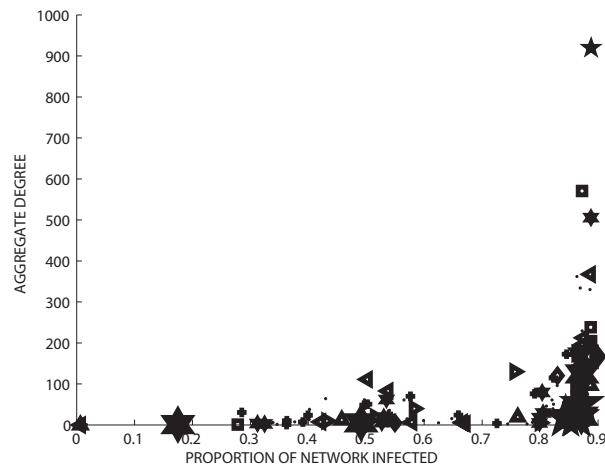

Fig. 13 Average degree versus infected proportion for $\beta = 1.0$.

5 Discussion

We are concerned here with quantifying properties of a time-dependent interaction network in terms of epidemic spread. Our results indicate that ranking nodes according to their broadcast centrality from [5] can operate as an accurate, and relatively inexpensive, proxy for more detailed rankings of their ability to spread infection based on averaging over microscale simulations. In particular, the results were insensitive to infection probability in the microscale model. By contrast, simply judging a node by its overall bandwidth does not provide a useful picture.

There are many avenues for extending this type of study. For example:

- Further investigation is needed to test whether improvements will arise from fine tuning the Katz-style downweighting parameter α used in the broadcast centrality measure, as a function of the infection probability, β.
- Other types of interaction data could be used to generate the underlying dynamic topology.
- The accompanying *receive centrality* measure from [5] can be tested as a proxy for the vulnerability of a node to infection.
- More complex compartmental epidemic models could be investigated, including SIS and SIR. In this case, our intuition is that the straightforward dynamic walk counting approach of [5] will be less successful, and hence new classes of time-respecting network centrality measures will be required.
- In addition to local node-based information, global summaries, such as an appropriate, dynamic, version of the basic reproduction number, R_0, could be compared with network features. A study of this type has recently been performed for the case of a static network in [1].

Acknowledgment

References

1. Ames, G., George, D., Hampson, C., Kanarek, A., McBee, C., Lockwood, D., Achter, J., Webb, C.: Using network properties to predict disease dynamics on human contact networks. Proc Biol Sci. **278**(1724), 3544–50 (2011)
2. Barrat, A., Cattuto, C.: Temporal networks of face-to-face human interactions. In: P. Holme, J. Saramäki (eds.) Temporal Networks. Springer (2013)
3. Carvalho, V.R., W.Cohen, W.: Recommending recipients in the Enron email corpus. Tech. Rep. CMU-LTI-07-005, Carnegie Mellon University (2007)
4. Estrada, E.: The Structure Of Complex Networks. Oxford Univerity Press (2011)

5. Grindrod, P., Higham, D.J., Parsons, M.C., Estrada, E.: Communicability across evolving networks. Physical Review E **83**, 046,120 (2011)
6. Katz, L.: A new index derived from sociometric data analysis. Psychometrika **18**, 39–43 (1953)
7. Lee, S., Rocha, L.E.C., Liljeros, F., Holme, P.: Exploiting temporal network structures of human interaction to effectively immunize populations. PLoS ONE **7** (2012)
8. Mantzaris, A.V., Higham, D.J.: Dynamic communicators. to appear in European Journal of Applied Mathematics (2012)
9. Nicosia, V., Tang, J., Mascolo, C., Musolesi, M., Russo, G., Latora, V.: Graph metrics for temporal networks. In: P. Holme, J. Saramäki (eds.) Temporal Networks. Springer (2013)
10. Rocha, L.E.C., Liljeros, F., Holme, P.: Simulated epidemics in an empirical spatiotemporal network of 50,185 sexual contacts. PLoS Comput Biol **7** (2011)
11. Tang, J., Leontiadis, I., Scellato, S., Nicosia, V., Mascolo, C., Musolesi, M., Latora, V.: Applications of temporal graph metrics to real-world networks. In: P. Holme, J. Saramäki (eds.) Temporal Networks. Springer (2013)
12. Tang, J., Mascolo, C., Musolesi, M., Latora, V.: Exploiting temporal complex network metrics in mobile malware containment. In: Proceedings of IEEE 12th International Symposium on a World of Wireless Mobile and Multimedia Networks (WOWMOM) (2011)
13. Tang, J., Musolesi, M., Mascolo, C., Latora, V., Nicosia, V.: Analysing information flows and key mediators through temporal centrality metrics. In: SNS '10: Proceedings of the 3rd Workshop on Social Network Systems, pp. 1–6. ACM, New York, NY, USA (2010). DOI http://doi.acm.org/10.1145/1852658.1852661
14. Tang, J., Scellato, S., Musolesi, M., Mascolo, C., Latora, V.: Small-world behavior in time-varying graphs. Physical Review E. **81** (2010)
15. Wasserheit, J.N., Aral, S.O.: The dynamic topology of sexually transmitted disease epidemics: implications for prevention strategies. Journal of Infectious Diseases **174** (1996)